Pharm Res (2014) 31:3461–3477
DOI 10.1007/s11095-014-1434-z

RESEARCH PAPER

Development of High Drug Loaded and Customizing Novel Nanoparticles for Modulated and Controlled Release of Paclitaxel

Primiano Pio Di Mauro • Salvador Borrós

Received: 14 February 2014 / Accepted: 3 June 2014 / Published online: 18 June 2014
© Springer Science+Business Media New York 2014

ABSTRACT

Purpose The objective of this study was to develop a custom-tailored polymeric drug delivery system for paclitaxel, employing a novel biodegradable block co-polymer (P), intended to be intravenously administered, capable of improving therapeutic index of the drug and devoid of the adverse effect of an uncontrolled release.

Methods Paclitaxel loaded nanoparticles (PTX-NPs) were prepared by a modified nanoprecipitation method and emulsification-solvent evaporation method. Our approach involves a focusing on the formulation parameters that can be modified in order to obtain completely customized NPs in terms of size, zeta-potential, drug content and release profile. The biocompatibility and anti-proliferative efficiency of PTX-NPs against glioblastoma cell line were evaluated *in vitro* by MTS.

Results All formulations showed spherical nanometric (<200 nm), monodisperse (~0.1), Poly (Ethylene Glycol) (PEG)-coated and negatively charged particles. Selected NPs revealed higher PTX content (up to 24%) in comparison with polyester-based NPs. The release behaviour of PTX from the developed NPs exhibited an approximately first-order profile, without initial burst and characterized by a slow and constant release. Hydrophobic character of the NPs can be set in order to achieve a slower and more controlled release for a prolonged period of time. PTX-NPs were hemocompatible and had significant *in vitro* anti-tumoral activity against human primary glioblastoma cell line (U-87 MG); cytotoxicity was in time- and drug concentration- dependent manner.

Conclusions The developed drug delivery system proved to be suitable for intravenous administration. NPs characteristics can be customized to obtain high PTX loaded NPs that can improve therapeutic index and avoid an uncontrolled release.

P. P. Di Mauro • S. Borrós (✉)
Sagetis-Biotech; Grup d'Enginyeria de Materials (GEMAT)
Institut Quimic de Sarria, Universidad Ramon Llull
Via Augusta 390, 08017 Barcelona, Spain
e-mail: salvador.borros@iqs.url.edu

P. P. Di Mauro
e-mail: pdimauro@sagetis-biotech.com

KEY WORDS anti-glioma · block co-polymer · controlled release · drug content · paclitaxel

INTRODUCTION

Cancer is the leading cause of death worldwide (1). Over the past few years the improvements in nanotechnology had a revolutionary impact on cancer diagnosis and therapy. Drug delivery systems offer novel therapeutic opportunities allowing controlled release of drugs that were previously unsuited to traditional oral or injectable formulations. An efficacious and targeted delivery minimizes side effects and improve therapeutic efficiency (2). In particular, current anticancer drug therapy results in systemic side effects due to nonspecific uptake by healthy tissues, thus limiting the administered dose (3). In the last years there has been an intensive research on the development of biodegradable NPs as a suitable means for controlled drug release and targeting (4). The major goals in designing NPs as a delivery system are to control surface properties, particles size, drug loading and release of pharmacologically active agent (5,6). Surface properties plays key role on the therapeutic efficacy of NPs. To minimize the adsorption of opsonins and thereafter the clearance from the blood, stealthy or long-circulating NPs are achieved by introducing flexible hydrophilic coating (7). Moghimi D. S. *et al.* have demonstrated that the effect of size on NPs biodistribution is non-linear and organ specific (8). This is due to physical and physiological barriers that systematically administered NPs encounter in organs (9). For a suitable *in vivo* biodistribution the size of NPs should typically be controlled at less than 200 nm with narrow polydispersities (10). An important parameter for NPs intended to use in clinical is drug loading (11). Indeed, at lower drug content, larger amounts of delivery vehicles need to be administered. To realize effective drug delivery, a controlled release profile is also important in order to achieve site-specific action of the drug at therapeutically

optimal rate and dosage regimen. Synthetic polymers, especially linear polyesters such as poly (ε-caprolactone) (PCL), polylactide (PLA) and poly (lactide-co-glycolide) (PLGA), have been widely utilized as the polymeric matrix materials of drug delivery systems (5,12,13). Many methods have been developed for preparing NPs; these methods can be divided into two main categories according as the formulation requires a polymerization reaction or is obtained by preformed polymer (14). The nanoprecipitation technique was first developed by Fessi and co-workers (15). This technique uses interfacial preformed polymer deposition followed by solvent displacement and the NPs formation is instantaneous and the entire procedure is carried out in only one step (16). PLA NPs typically prepared via nanoprecipitation (5) tend to give NPs with various formulation challenges that remain to be addressed. Moreover, PLA NPs typically show "burst" drug release profiles in aqueous solution, with 80–90% of the encapsulated drug rapidly released during the first few hours (17). Biodegradable NPs have been used as sustained release vehicles for administering active agents such as natural or synthetic organic or inorganic entities, proteins, peptides and nucleic acids. The active agent is either dissolved, entrapped, encapsulated, or attached to the NPs matrix (18). Among the encapsulated drugs, PTX is one of the successful chemotherapeutic agents and it has been approved to effectively kill a wide variety of solid tumors. However, the difficulties in clinical applications are due to the poor water solubility. Commercial formulation of PTX for clinical treatment is constituted with ethanol and Cremophor EL, which has been associated with acute hypersensitivity reaction (19) and side effects including neutropenia, cardiac arrhythmias, dose-related myalgia, neuropathy and serious killing of normal cells (20). To achieve desired therapeutic performance of PTX, various formulations were proposed, among them liposomes, which can reduce the side effects but also have some disadvantages such as low entrapment efficiency (21). In this work, a novel biodegradable block co-polymer (P) was synthetized to develop a long circulating drug delivery system for anticancer drugs. A precise correlation between NPs characteristics and different experimental parameters was found so as to obtain completely customized NPs in terms of size, zeta-potential, drug content and release profile. The work is carried out using lipophilic drug PTX, with the aim to obtain a very monodisperse NPs population in which NPs could be equipped with an optimal external hydrophilic coating (PEG-corona). The drug encapsulation capability as well as *in vitro* release kinetics from NPs were also investigated revealing that a considerable quantity of drug can be loaded; furthermore, depending on the PTX payload, hydrophobic character of the NPs can be set in order to achieve a slower and more controlled release for a prolonged period of time. The biocompatibility and anti-proliferative efficiency of PTX-NPs against glioblastoma cell line were evaluated *in vitro* by MTS.

MATERIALS AND METHODS

Materials

1.8-Octanediol (98%) and PEG (M_w 1.5 KDa) were purchased from Sigma (USA). Glutaric acid (99%) was obtained from Alfa Aesar (USA). PTX (≥97%) was provided by Yunnan Hande Bio-Tech CO, LTD, P.R. China. FBS was purchased from Lonza, L-Glutamine and Penicillin/Streptomycin were provided by Labclinics. All other chemicals of analytical grade were purchased from Sigma (Sigma–Aldrich, Germany).

Synthesis of Block Co-polymer (P)

Block co-polymer (P) constituted by rigid and flexible alternating blocks was synthetized by the esterification of 1.8-Octanediol with glutaric acid and subsequently with PEG 1500. Glutaric acid (6 g, 45 mmol) and 1.8-Octanediol (5.53 g, 37 mmol) were reacted in a microwave reactor (Discovery CEM) at a power of 100 W for 1 h. The reaction was performed under vacuum (100 mbar) with continuous stirring and cooling the system with compressed air to maintain the temperature constant at 120°C. Once the glutaric acid exceeding prepolymer or rigid block was generated, it was subsequently reacted with PEG 1500 which is added in a 1:1 weight ratio with the prepolymer. The polymerization reaction was performed in the microwave reactor with the conditions above described. The resulting block co-polymer (P) was dried at room temperature and used for NPs preparation without further treatment.

Characterization of Block Co-polymer (P)

To determinate the molecular structure of block co-polymer P a Fourier Transform Infrared (FTIR) analysis was performed using a Thermo Scientific Nicolet iS10 spectrophotometer. The composition of the P co-polymer was determined by proton nuclear magnetic resonance ^{1}H-NMR in $CDCl_3$ at 300 MHz (Varian 400 MR). The weight-averaged molecular weight and molecular weight distribution of the obtained polymers were determined using a gel permeation chromatography (GPC) LaChrome Elite from Hitachi, with pump and refractive index (RI) detector from Hitachi. The following conditions were adopted: the column was Shodex KF-603, the mobile phase was THF HPLC grade, and flow rate was 0.5 ml/min. The samples were dissolved in THF, filtered, and then 20 μl were injected. The molecular weights of the copolymers were determined relative to the standards curve, prepared using a series of Shodex SM-105 polystyrene standards.

Formulation of NPs

NPs were prepared according to a modified nanoprecipitation method (or solvent displacement method) (15). 20 mg of P and

a specified quantity of PTX were dissolved in acetone, a suitable organic solvent pharmacologically accepted with regard to toxicity, to form the diffusing phase. This phase was then added to dispersing phase in which the polymer is insoluble, by means of a syringe, controlled by a syringe-pump (KD scientific), positioned with the needle directly in the medium, under a magnetic stirring of 120 rpm and at room temperature. The resulting NPs suspension was allowed to stir uncovered at room temperature until complete evaporation of the organic solvent. Drug free NPs were prepared according to the same procedure. To investigate the influence of formulation parameters on NPs formation, size and zeta potential the following variables were studied:

- methanol, ethanol and water were used as dispersing phase (no-solvent)
- for each no-solvent, the ratio S/NS was varied from 1:2 to 1:20 (v/v)
- polymer concentration in the organic phase was increased from 10 to 50 mg/ml
- a range of drug dissolved in the organic phase (theoretical drug loading) from 0 to 25% was used.

In each set of experiment only one formulation variable was changed at a time while the other parameters were kept constant. The NPs were processed as above in triplicate.

Separation of Free from Incorporated Drug

NPs were purified by centrifugation (Hettich Centrifuge, EBA 21, 4,000 g, 45 min.) with ultra-centrifugal device (Amicon Ultra-15, Ultracel membrane with 100,000 MWCO, Millipore, USA). The supernatant containing the dissolved free drug was discarded and the pellet freeze-dried (Telstar, LyoAlfa 6) for 48 h. Freeze-drying was carried out without lyoprotectant. The nanoparticle recovery was calculated using Eq. (1)

$$\text{NPs recovery (\%)} = \frac{\text{Mass of NPs recovered} \times 100}{\text{Mass of polymer and drug used in formulation}} \quad (1)$$

Characterization of PTX-Loaded-NPs

Determination of NPs Size and Polydispersities

The NPs size distributions and polydispersity were measured by Dynamic Light Scattering (DLS) (Malvern Zeta Sizer Nano Series) at 25°C and at scattering angle of 90° using sample appropriately diluted with mQ water. For each sample the intensity-weighted mean value was recorded as the average of three measurements. The results were expressed as mean ± S.D for two replicate sample. Further measurements were performed by Nanoparticles Tracking Analysis (NTA) (Nanosight LM 10, Laser Module LM 14C), with a 532 nm laser beam passed through a prism-edged optical flat and validating all data with video files of the NPs moving under Brownian motion to determinate NPs size distribution and monodispersity.

Surface Charge and Morphology

NPs were also characterized with respect to zeta (ζ) potential, the analysis was performed in triplicate on Malvern ZetaSizer (Nano Series) with a Smoluchowsky constant F (K_a) of 1.5 to achieve zeta potential values from electrophoretic mobility. For each sample the mean zeta potential was recorded as the average of three measurements. The results were expressed as mean ± S.D for two replicate sample. The size and morphology of the NPs were observed by Transmission Electron Microscopy (TEM) (Jeol Jem 2011). A drop of the NPs suspension (10 μl) was placed on carbon electron microscopy grids (Holey Carbon Film) and air-dried before analyze at an acceleration voltage of 200 kV without negative staining.

Thermal Characterization

The physical state (crystalline *versus* amorphous) and miscibility of PTX in the NPs were characterized by Differential Scanning Calorimetry (DSC) (Mettler Toledo DSC821e) on the glass transition temperature (T_g) or melting point (T_m). As a control pure PTX, empty NPs and the physical mixture of PTX with empty NPs (1:1 w/w) was also analyzed. Approximately 4–5 mg of each sample, sealed in a standard aluminum pan, was purged with dry nitrogen at a flow rate of 50 ml/min while the sample was heated from 50 to 300°C at a rate of 10°C/min.

Drug Incorporation Efficiency

Freeze-dried NPs loaded with PTX were dissolved in acetonitrile and the amount of entrapped drug was detected by Ultra Performance Liquid Chromatography (UPLC) (Waters ACQUITY UPLC H-Class). A reverse phase BEH C18 column (1.7 μm 2.1×50 mm) was used. The mobile phase consisted of a mixture of acetonitrile and water (60:40 v/v) and was delivered at a flow rate of 0.6 ml/min. PTX was quantified by UV detection (λ=227 nm, Waters TUV detector). A calibration curve of standard PTX solution was used to obtain the PTX concentration, which was linear over the range of 60.5–0.47 μg/ml with a correlation coefficient of R^2=0.9998. Drug incorporation efficiency was expressed as drug content (D.C. % w/w) and encapsulation efficiency (E.E. %); represented by Eqs. (2) and

(3), respectively. For each sample the mean value was recorded as the average of three measurements. The results were expressed as mean ± S.D for two replicate.

$$\text{Drug Content}\left(\%\frac{w}{w}\right) = \frac{\text{Mass of drug in NPs} \times 100}{\text{Mass of NPs recovered}} \quad (2)$$

$$\text{Encapsulation Efficiency}(\%) = \frac{\text{Mass of drug in NPs} \times 100}{\text{Mass of drug used in formulation}} \quad (3)$$

In Vitro Drug Release Analysis

In vitro drug release from PTX loaded NPs was performed using a modified dialysis-bag diffusion technique, as reported by Kim *et al.* and Averineni *et al.* (22,23). Specifically, a known amount of freeze-dried PTX-NPs, corresponding to 0.3 mg of PTX, was suspended in a dialysis bag (regenerated cellulose tubular membrane, Cellu SEP® T2, nominal MWCO 6000–8000, membrane filtration products, Inc, TX) containing 15 ml of release PBS solution (0.1 M at pH 7.4 and 0.3% v/v of Tween-80). The bag containing NPs suspension was placed in a 50 ml Eppendorf® Tube (Fisher Scientific Company, Houston, TX) containing 30 ml of release medium (PBS solution and 0.3% v/v of Tween-80). The whole system was then placed in an orbital shaking incubator (LM-450D, Yihder Co., Ltd) at 37°C and at shaking speed of 200 rpm. At pre-decided time points 1 ml aliquots of release medium was withdrawn and replaced with an equal volume of fresh medium to maintain the sink conditions. The withdrawn aliquots were filtered through a 0.2 μm syringe filter directly into UPLC vials and immediately capped. The amount of PTX released in each time interval was determined by UPLC with a reverse phase BEH C18 column (1.7 μm 2.1×50 mm). The mobile phase consisted of a mixture of Acetonitrile/Ammonium Acetate Buffer (20 mM, pH 4.5)=60/40 delivered at a flow rate of 0.6 ml/min. PTX was quantified by UV detection (λ=227 nm, Waters TUV detector); the reported values are averages ± S.D. of three replicates. The percent drug release was calculated as percentage of the total encapsulated drug. For the polymer degradation studies an UPLC (Waters ACQUITY UPLC H-Class) equipped with a TOF-MS detector was used, using the same UPLC conditions above described.

Cell Experiment

In Vitro Immunological Assay

Hemocompatibility of PTX-NPs was evaluated diluting NPs in PBS (0.1 M pH 7.4) at concentrations of 10 and 100 μg/ml. Hemocompatibility test was carried out after blood exposure. Interaction of NPs with blood was analyzed using normal human plasma collected under citrate 15 min before starting blood exposure during 15 min at 37°C and at atmospheric pressure. First analysis was the hemolysis test and according to Drabkin's method, when free hemoglobin <2% NPs were considered non haemolyitic; 2–5% slightly haemolytic and >5% haemolytic. Further experiments were blood cell counting and quantification of complement activation adopting the determination of the C3a concentration (ELISA kit). Finally, analysis of the activation of the coagulation either by the intrinsic (TCA test) or the extrinsic (Quick) pathways was performed.

In Vitro Anti-proliferative Efficiency

In order to evaluate the cytotoxicity of the PTX-NPs on U-87 MG cells, the cells were grown in DMEM supplemented with 10% FBS, 1% L-Glutamine and 1% Penicillin/Streptomycin and plated in 96-well plates at a cellular density of 30.000 cells/ml. After 24 h, medium was aspirated and substituted with 100 μl of various PTX concentration (10, 20 nM) of 3, 5 and 8% theoretical loaded PTX-NPs suspensions. Empty NPs were also examined with the concentration corresponding to that of 10 nM of PTX. One column, cells with PTX at 10 and 20 nM, was used as positive control; one column, cells without NPs, was used as the control; another column, without cells, was used as the blank. After 1, 4, 6, 8 and 11 days, cell viability was assessed via MTS (CellTiter 96® AQueous One Solution Cell Proliferation Assay, Promega Corporation, USA) following the manufacturer instructions. Briefly, cells were washed with PBS and incubated with a solution of the MTS reagent and complete media at 37°C. The absorption (A), which represented cell viability was measured via a microplate reader (Spectramax M2^e) at the wavelength of 490 nm. Cell viability was calculated by Eq. (4) and the errors bar were obtained from triplicate samples.

$$\text{Cell viability } (\%) = \frac{A_{sample} - A_{blank}}{A_{control} - A_{blank}} \times 100 \quad (4)$$

Emulsion-Based PTX Loaded NPs

To demonstrate the capability of block co-polymer P to be employed as a drug delivery system, NPs were also prepared by a modified emulsification by sonication-solvent evaporation (24). This method involved the use of an organic phase consisting of polymer at 10 mg/ml concentration and selected amounts of PTX, dissolved in 1 ml DCM. This organic phase was added to an aqueous phase to form an emulsion, which was broken down into nanodroplets by applying external energy through a 10 s pulsing (2″on/2″off) sonication at 100% amplitude. Upon the solvent evaporated whit magnetic

stirring at 300 rpm and under atmospheric conditions for 4 h, a colloidal suspension of PTX-NPs was obtained. NPs were purified as described above and freeze-dried with cryoprotectant to ensure optimal re-suspension.

Statistical Methodology

Data for all experiments were expressed as means ± SD. The significance of differences was assessed using Student's *t*-test, and was termed significant when $P \leq 0.05$.

RESULTS AND DISCUSSION

Synthesis and Characterization of P Co-polymer

Block co-polymer P constituted by flexible blocks (PEG 1500) and rigid blocks (1.8-Octanediol and Glutaric Acid), was synthetized by polycondensation in a microwave reactor, under vacuum, at 120°C and 100 W (Fig. 1). The identity and purity (with respect residual monomers) of the co-polymer P were determined by FTIR. Figure 2 shows a representative FTIR spectrum of P, which is consistent with the structure of the expected polymer. It shows that the strong band at 1,732 cm^{-1} is assigned to C=O stretch of the ester band. The absorption band at 3,449 cm^{-1} is attributed to the terminal hydroxyl group and that at 1,500–1,045 cm^{-1} is due to the C–O stretching of the ester band. C-H stretch of CH_2 is observed at absorption band 2,919–2,850 cm^{-1}. The composition of P co-polymer is confirmed by ^{1}H-NMR (Fig. 3). One of the prominent features is a large peak at 3.64 ppm (peak b), corresponding to the methylene groups of the PEG 1500. The multiplets at 4.06 and at 1.61 ppm (peak a and e) correspond to the CH_2 protons of 1.8-octanediol. The multiplets at 2.37 and 1.94 ppm (peak c and d) are assigned to the glutaric acid methylene protons in α and β position relative to carbonyl group, respectively. The weight-averaged molecular weight and molecular weight distribution of the obtained prepolymer and P co-polymer were determined by means of GPC. The molecular weight were found to be 1,069 and 2,335 for the prepolymer and P co-polymer, respectively. The PDI was narrow, which was around 1.8 for the prepolymer and 2.01 for the P co-polymer.

Preparation and Characterization of NPs

Effects of Varying Formulation Parameters to Control NPs Size and Zeta Potential

NPs with and without PTX loading and based on different formulation parameters were prepared by a modified nanoprecipitation method (15). An experimental design of NPs fabrication was selected to investigate how formulation variables (no-solvent type, solvent/no-solvent ratio and polymer concentration) could affect NPs characteristics. The experiments were designed with the ultimate goal of tailoring NPs in terms of size and zeta potential. As a starting point for controlling NPs characteristics, we first studied the effect of different no-solvent types used to disperse organic phase. Senichev *et al.* have demonstrated that a solvent/no-solvent (S/NS) system affects the diffusion rate and thus the NPs size (25). To analyze the impact of a S/NS system we studied the affinity of the solvent (acetone) for the no-solvent by means of the interaction parameter (χ). This interaction is expressed as:

$$\chi = \frac{V_{NS}}{RT}(\delta_S - \delta_{NS})^2 \quad (5)$$

Where V_{NS} is the molar volume of the non-solvent (here, methanol 40.7 cm^3/mol, ethanol 58.5 cm^3/mol and water 18.016 cm^3/mol) and δ is the Hildebrand solubility parameter. The calculated interaction parameters (Table I) were then plotted against NPs size and presented in Fig. 4. As expected, the higher the interaction parameter, the larger the NPs. We chose to investigate the relationship between NPs size and S/NS miscibility and observed a dependence of NPs size on the solubility parameter. As shown in Fig. 5 an increase of S/NS miscibility (decrease in Δδ, as indicated by the arrow shown in Fig. 5) led to a decrease in the mean NPs size, with all other formulations parameters held constant.

Concurrently with the investigation of the effect of S/NS, we studied the effect of altering the S/NS ratio during nanoprecipitation. When the ratio of diffusion of the acetone into the non-solvent was varied for a fixed polymer concentration (Fig. 5), a correlation of NPs size with S/NS ratio was observed. This correlation was remarked for all polymer concentrations and for two of the non-solvent types tested (Fig. 6). In water, for example, at 10 mg/ml polymer concentration, NPs size increased from 116.5±0.9 to 174.4±1.2 nm as the ratio S/NS decreased from 0.5 to 0.05, respectively (mean ± SD, $n=3$ for each formulation; $p>0.05$). For methanol the correlation is inverse than water, it was found that the higher solvent/non-solvent ratio, the bigger NPs; for example, at 50 mg/ml polymer concentration, NPs size decrease from 125.4±1.7 to 73.63±0.15 nm as the ratio S/NS decrease from 0.5 to 0.05, respectively. For the ethanol, no clear correlation between the NPs size and S/NS ratio was found. On the other hand, a clear dependence of the NPs size from polymer concentration in the diffusing phase, was observed for all the non-solvent types tested. When polymer concentrations were varied during NPs fabrication at a fixed S/NS ratio, an increasing NPs size with increasing polymer concentration is observed (Fig. 6). For example, at 1:10 acetone/ethanol ratio, NPs sizes were 84.8±2.5, 102.7±0.47, 134.8± 1.7 nm when the polymer concentration were 10, 20,

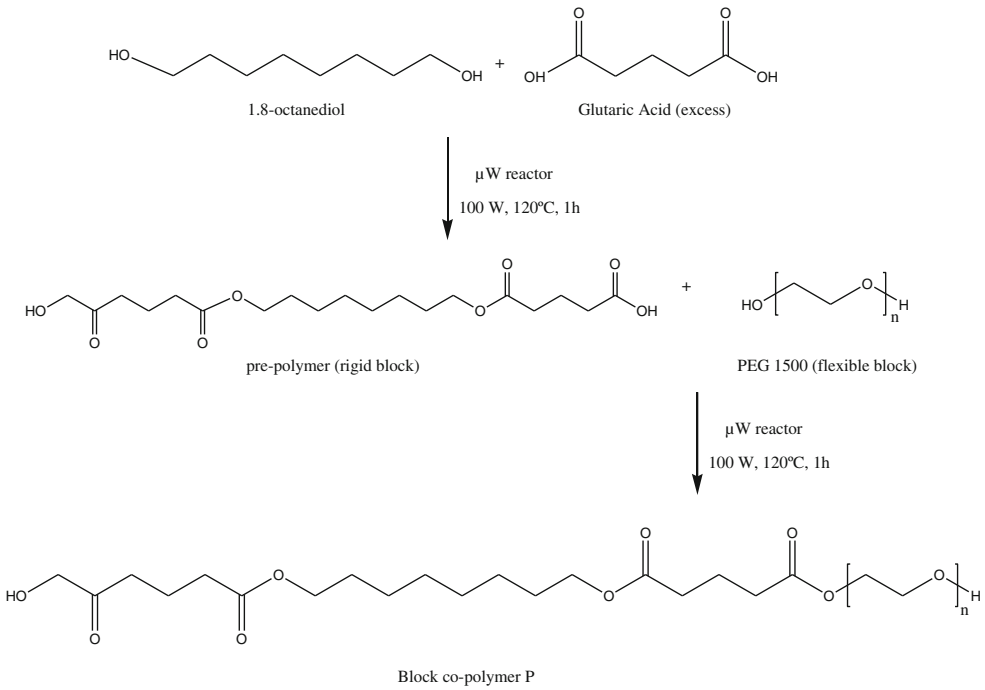

Fig. 1 Schematic diagram of the synthesis of block-co polymer P by polycondensation.

50 mg/ml, respectively. Similar trends were observed in all other solvents investigated. Regarding polymer concentration has to be taken into consideration that a too high polymer concentration in the solvent prevented nanoprecipitation. This effect is probably due to the high viscosity of the polymeric solution that prevents an appropriate diffusion of the

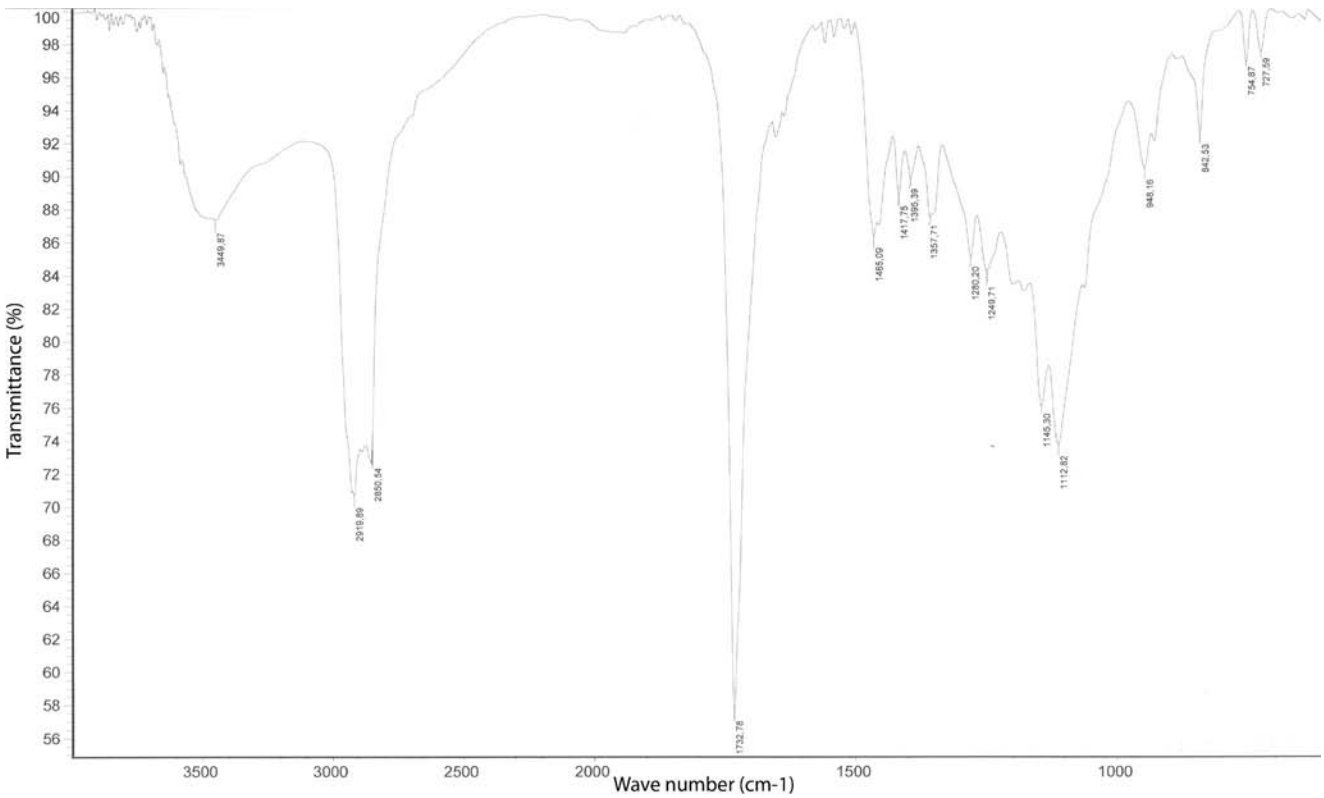

Fig. 2 FTIR spectra of the P co-polymer.

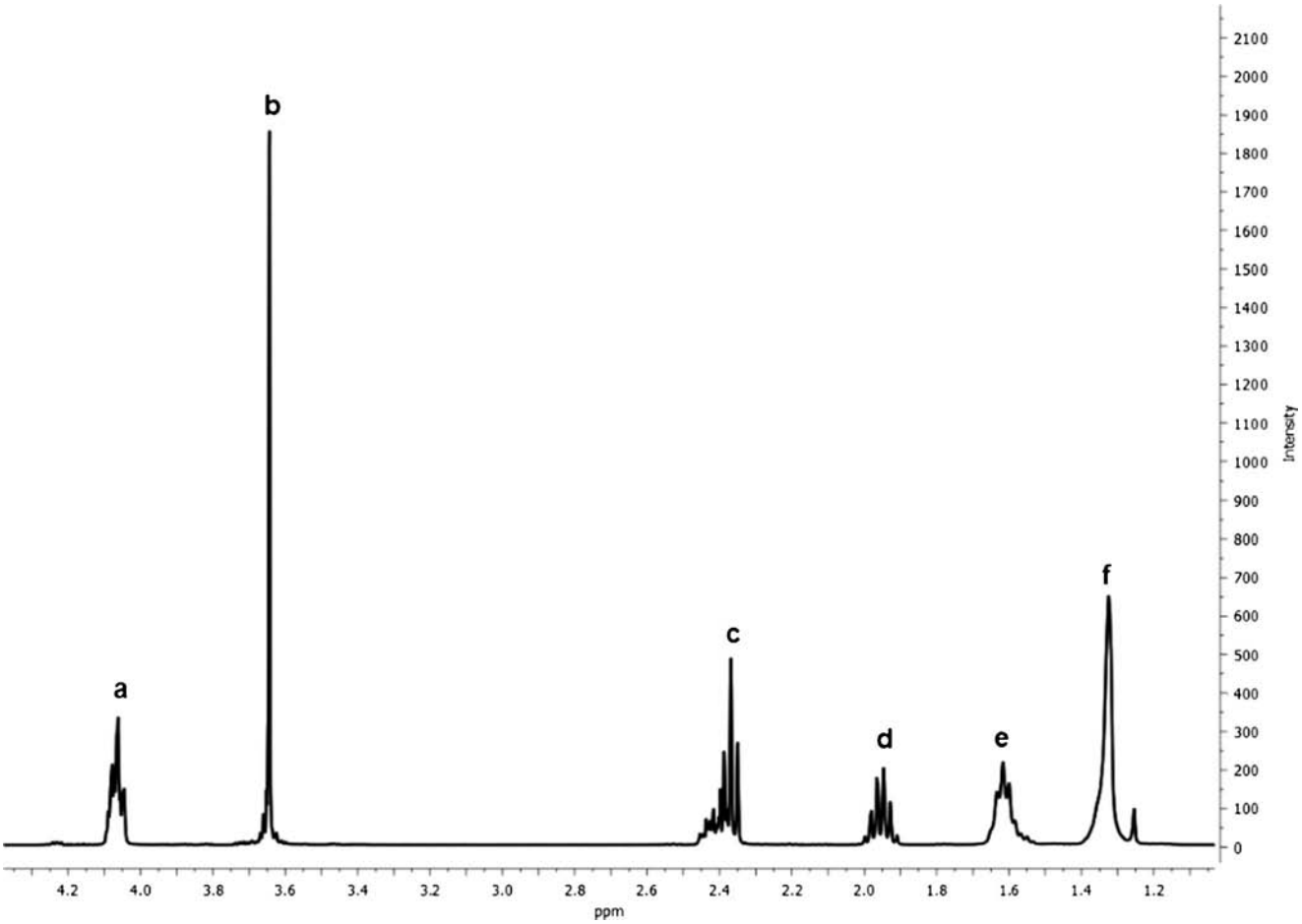

Fig. 3 ^{1}H-NMR spectra of P co-polymer in CDCl3.

solvent toward the non-solvent. Other authors found also that the higher the polymer concentration in the solvent, the higher loss of polymer; they explained this effect in terms of the intrinsic viscosity and interaction constants (26). Also we studied the effects of varying formulations parameters on ζ potential. This is an important index for the stability of the NPs suspension. High absolute value of zeta potential indicates high electric charge on the surface of the NPs, which can cause strong repellent forces among particles to prevent aggregation (27). All NPs batches were found negatively charged with a value depending on the S/NS ratio and polymeric concentration. As shown in Fig. 6 the zeta potential ranged ~20 mV for water, ~12 mV for methanol and ~7 mV for ethanol. A clear correlation of ζ potential with formulation parameters was found for water; for a fixed polymer concentration, the lower the ratio S/NS, more negative the zeta potential. When polymer concentration were varied during NPs fabrication at a fixed S/NS ratio, it was found that the higher polymeric concentration, less negative NPs. Higher negative value (−32 mV) was obtained at 10 mg/ml polymeric concentration and 1:20 S/NS ratio. Methanol exhibited the same correlation with ζ potential values moving in a narrow range. Lower negative value (−5 mV) was obtained at 50 mg/ml polymeric concentration and 1:2 S/NS ratio. As though for the size, no clear correlation between zeta potential and formulation parameters was found for ethanol. A ζ potential in this range is often observed in polyester nanoparticles and a value of about − 25 mV ensures a high-energy barrier that stabilizes the nanosuspension (28).

Table I Non-solvent Miscibility Properties and Calculated Interaction Parameters χ of Solvent/Non-solvent Binary Mixture

Non-Solvent	Solubility parameter, δ $(MPa)^{1/2}$	Δδ	Interaction parameter[a,b] χ
Water	48	28.3	5.14
Methanol	29.7	10	1.44
Ethanol	26.2	6,5	0.87

[a] Solvent: Acetone

[b] Calculated using Eq. (5) and for T = 25°C (298 K). Polymer was not take into account

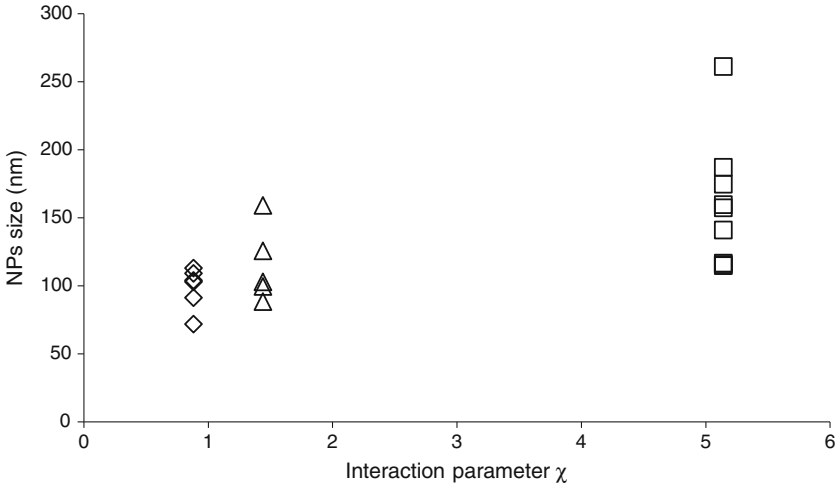

Fig. 4 Relationship between calculated interaction parameter χ of binary S/NS mixture and NPs size (◊ Ethanol, Δ Methanol, □ Water). NPs size determined by DLS.

Size Distribution and Zeta Potential

All formulations formed monomodally distributed NPs in the desire range below 200 nm (Fig. 6). The NPs size for all three non-solvent and for the investigated concentrations ranged from 70 to 200 nm and the size distribution was narrow with polydispersity in the range from 0.05 to 0.282. All formulations exhibited a net negative charge with ζ potential values ranging from −32 to −3 mV (Fig. 6).

Optimized Nanoprecipitation Variables

The initial approach to obtain PTX loaded NPs involved the choice of acetone and water as components of our nanoprecipitation based system. Acetone is not a concern in terms of toxicity, it belongs to Class 3 according to the ICH solvent toxicity scale (Class 3 solvent present very low risk to human health). Acetone has a low dielectric constant value which destines it a rather lipophilic drug encapsulation. The use of water as diffusing phase is the most appropriate; indeed the presence of the residual solvent is minimized only to residual acetone. In the following studies, the polymer concentration was fixed at 20 mg/ml with acetone/water ratio as 1:20. The optimized NPs were further investigated by NTA and DLS. PTX-NPs size distribution is rather monodisperse with a mean of about 180 nm, confirmed by NTA (Fig. 7a, c) and by DLS (Fig. 7b). No influence was exerted by PTX on the ζ potential value of NPs (−26 mV).

Surface Morphology

The morphology images of the 3% PTX-NPs obtained from TEM indicate that the NPs can be estimated around 130–180 nm in size and are spherical in shape with a smooth surface. In the TEM photos, "PEG corona" on the NP surface could be observed (Fig. 8). A further confirmation of the PEG corona surrounding NPs (marked in Fig. 8c with white arrow) was obtained by tilting angle experiments. The TEM carbon grid was tilted from 0° (Fig. 8c) to 45° (Fig. 8d); the PEG corona thickness remained unchanged, excluding a hypothetical aberration caused by the electrons beam interaction with the spherical surface (aberration occurred for the carbon grid spot marked with black arrow in Fig. 8c). An optimal external hydrophilic coating can improve stealthy behavior avoiding recognition by the reticuloendothelial system.

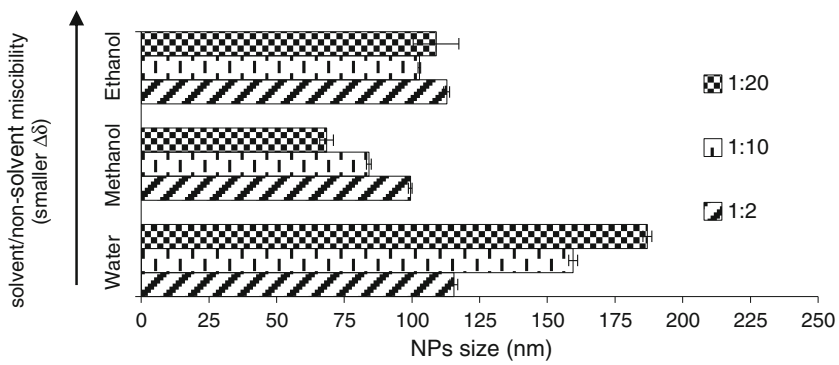

Fig. 5 Effect of varying formulation parameters on NPs size: modifying the non-solvent type and the acetone/non-solvent ration (1:2, 1:10, 1:20). NPs size determined by DLS; data represented mean ± SD ($n = 3$).

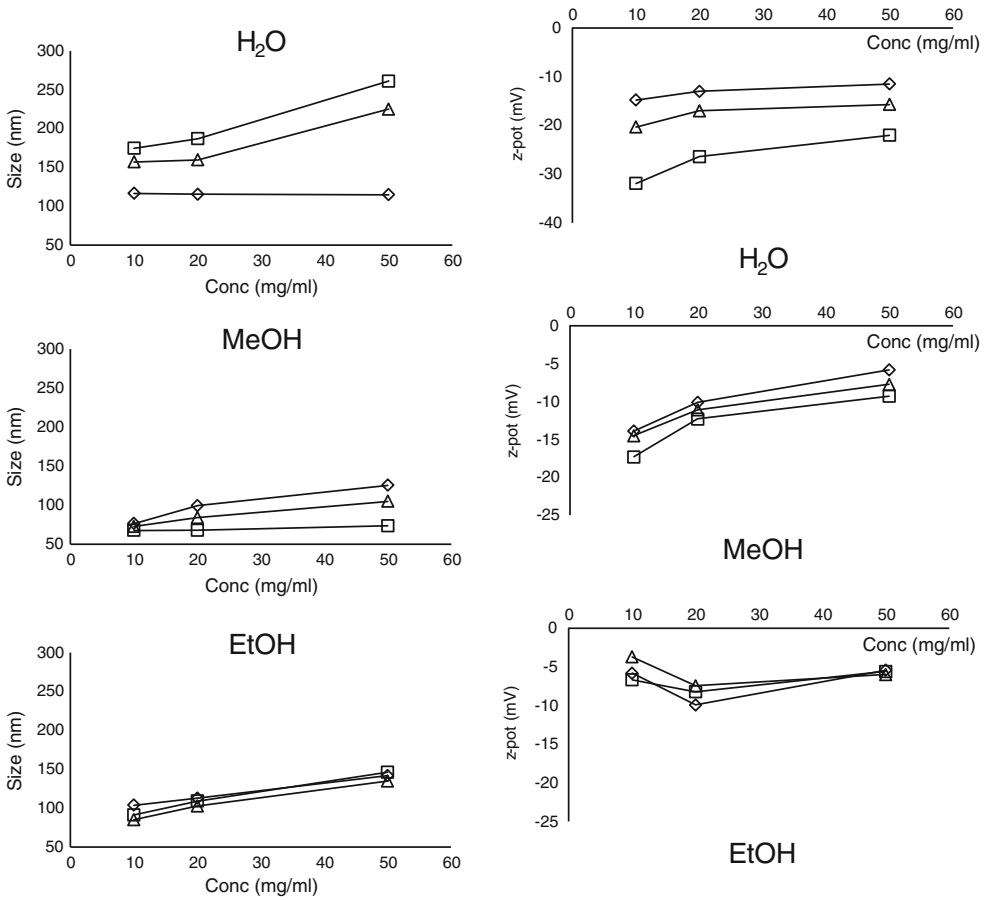

Fig. 6 Correlation of polymer concentration with NPs size (*left column*) and zeta potential (*right column*) at different solvent/non-solvent ratio (□ 1:20, Δ 1:10, ◊ 1:2) and for three non-solvent type. NPs size and z-potential determined by DLS; ($n = 3$, errors bar not shown, SD ≤ ±2.5 nm for size and ≤ ± 1.8 Mv for ζ).

Drug Incorporation Efficiency

The influence of the theoretical loading of PTX into P co-polymer NPs was examined. An increase in the theoretical loading from 2 to 20% w/w led to a corresponding increase in drug content from 3.8±0.2 to 24±3.5% w/w (Fig. 9). Along with drug content, encapsulation efficiency was analyzed and as shown in Fig. 9, the encapsulation efficiency remains constant approximately at 63±0.7% with increasing theoretical PTX loading. Our results are consistent with those reported by Danhier *et al.* (29), where 70% PTX E.E. into PLGA NPs was obtained with the nanoprecipitation methods. The results of this study are encouraging, because the drug contents are much higher than other polyester-based NPs (30). Generally, it was reported that the D.C. of PTX was about 3% in the nanoprecipitated NPs when the initial PTX loading was 4% (w/w) (30). Emulsioned PEG-PLA NPs reported by Q. Hu *et al.* (31,32) reach a drug content ranging from 1 to 3% along with an encapsulation efficiency of about 50%. When PLGA NPs are emulsioned with TPGS, which act as an emulsifier enhancing emulsification efficiency, PTX E.E. increases up to 80%, otherwise PTX D.C. does not exceed 3% (33).

As shown in Table II moderate NPs recovery yield after freeze-drying was achieved, ranging from 47.5±6.1 to 64.5±7% for lower and higher theoretical PTX loading, respectively.

We hypothesize that high D.C. and PTX depending NPs recovery yield, are most likely due to the arrangement of the hydrophobic P co-polymer regions when forming NPs. Indeed, PTX acting as binding agent facilitates nanoprecipitation probably by increasing lipophilic interaction among hydrophobic P co-polymer blocks. Supposedly, polyester regions of the P co-polymer are in close contact to PTX while PEG groups are directed to NPs surface to interact with water.

DSC

To determinate the physical status of PTX inside NPs, DSC analysis was performed. The results are shown in Fig. 10. Pure PTX showed an endothermic melting peak at about 223°C, shifted to lower temperature (210°C) in the thermograph of the physical mixture. Three percent PTX-NPs did not show a melting peak, such as the free-drug NPs, demonstrating that the polymer inhibited the crystallization of PTX during NPs formation. Therefore, it could be assessed that the PTX in the NPs was in an amorphous or disordered crystalline phase of a molecular dispersion or a solid solution state in the polymer

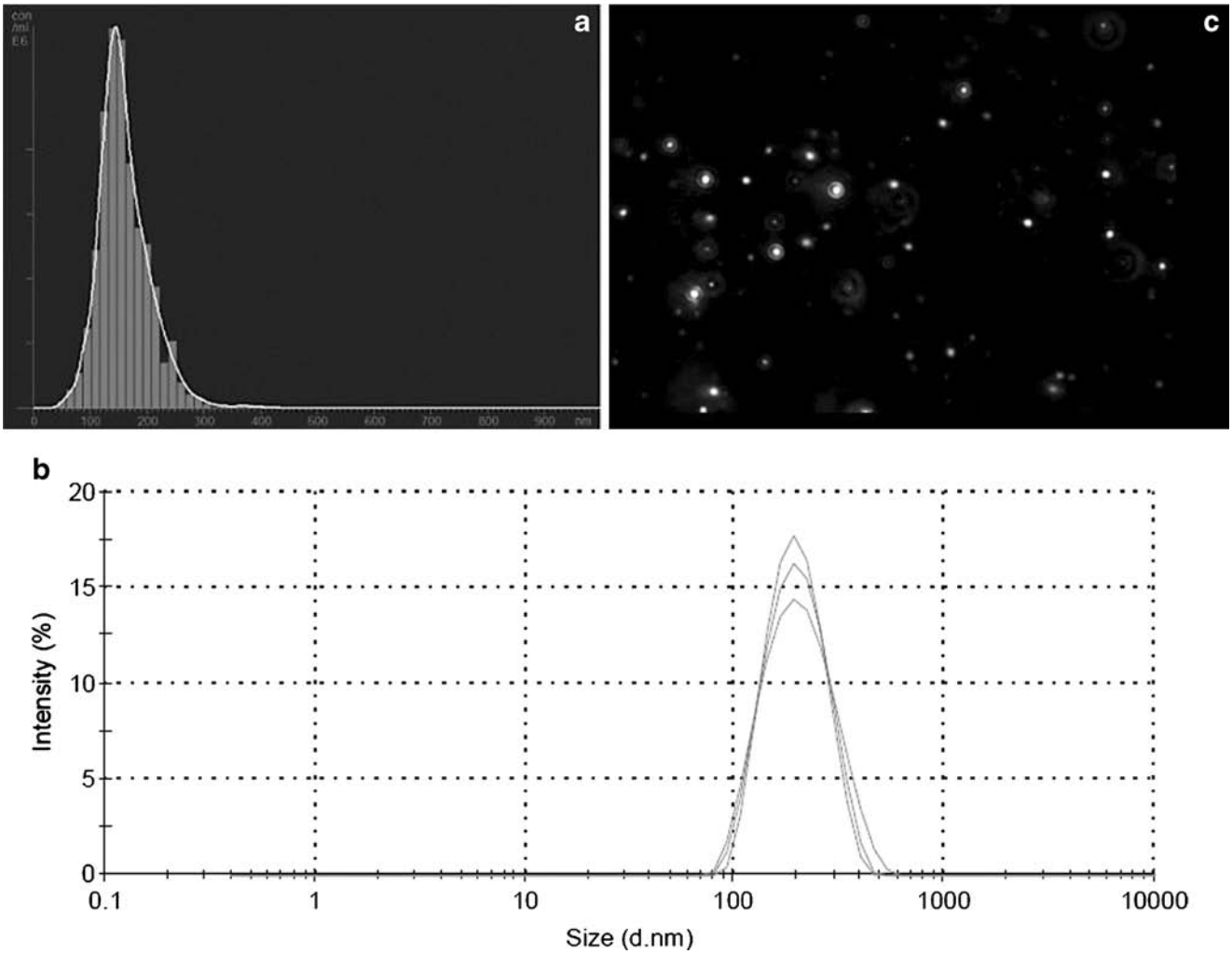

Fig. 7 PTX-NPs size distribution plots obtained by (**a**) NTA, (**b**) DLS and (**c**) NTA sample video frame of NPs moving under Brownian motion.

matrix after the production. Increasing NPs drug content, PTX remains in amorphous phase for theoretical drug loading of 5%. The 15% PTX-NPs showed a sharp melting peak at about 230°C indicating that a fraction of PTX was crystalline and did not dissolve in the P co-polymer matrix. Therefore, while PTX in the 3 and 5% sample completely dissolved in P co-polymer matrix, phase separation between PTX and P co-polymer occurred for the 15% PTX-NPs sample. Our results are consistent with previous findings by Mu *et al.* (34) that phase separation and crystallization of hydrophobic drugs like PTX can occur in NPs at high drug loading.

In Vitro Drug Release from PTX-NPs

The release profile of PTX from different formulations are presented in Fig. 11. For the different PTX loaded co-polymer NPs, the release pattern displayed an approximately first-order release, without initial burst and with a drug release reaching completion in approximately 12 days for 3% PTX-NPs. Figure 11 also shows PTX release profile in the first hours of test; it's possible to appreciate that the release is very slow and constant with approximately 6.2% of PTX released in 3 h from 3%-PTX-NPs. NPs with higher drug loading (10, 15%) showed the same trend with a slower release and around of 60% of PTX was released in 12 days. Since NPs are prepared by the same co-polymer P, the difference in PTX percentage released can be explained as follows. For 10 and 15% PTX loaded NPs, a considerable amount of drug is present in the bulk. This higher PTX content (w/w) in the polymeric matrix consequently bestow on NPs greater hydrophobic character, leading to slower release. Moreover the initial burst absence and the nearly linear behaviour demonstrate the absence of adsorbed drug on NPs surface. *In vitro* PTX release from polyester-based NPs usually present biphasic profile or very fast complete drug release. PHA (Poly Hydroxyalkanotes) and poly ε-CPL for example, released over 50% of PTX in the first hours (30,35). On the other hand PDLLA/PLGA PEG NPs exhibited a lower burst effect, but nevertheless the total cargo is released in 2 and 4 days, respectively (30,32), which, generally, is too fast to meet

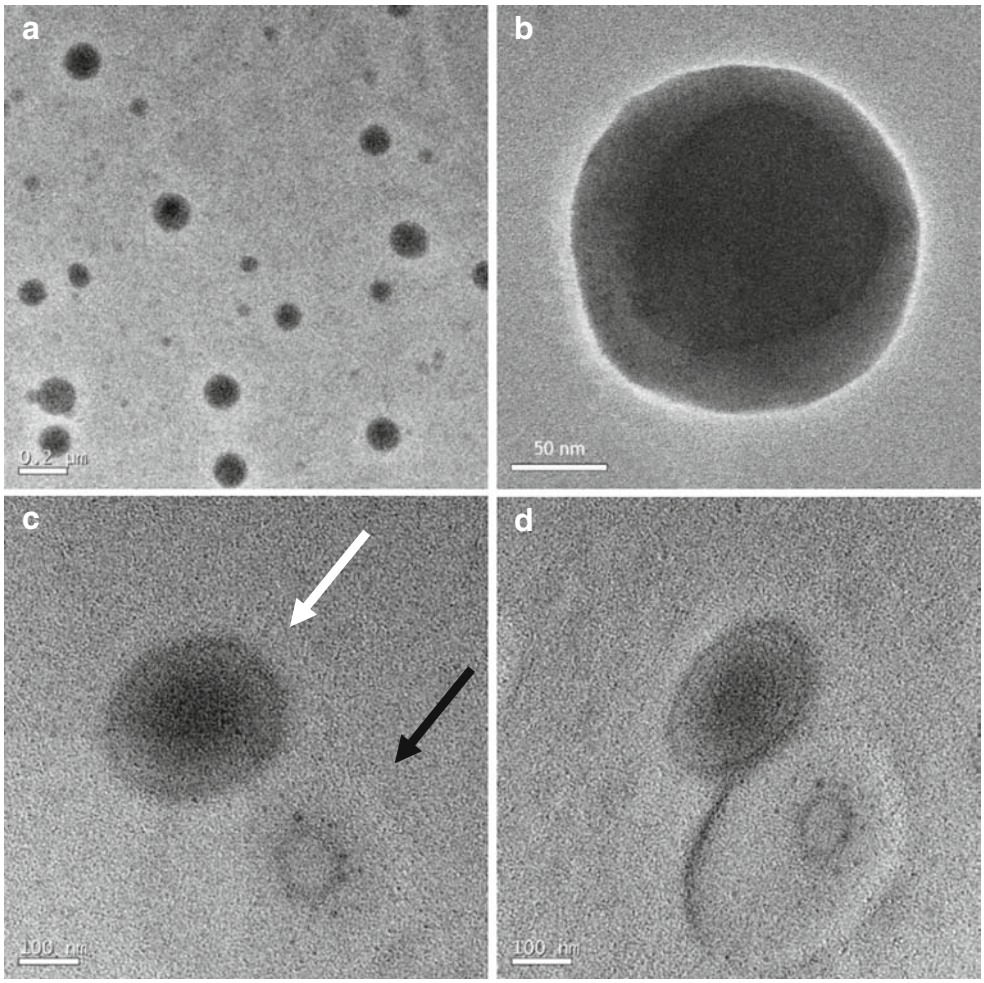

Fig. 8 TEM images of (**a**, **b**) PTX-NPs at different magnification and (**c**, **d**) PTX-NPs (*white arrow*) subjected to tilting angle experiments to assert PEG corona thickness remained unchanged; TEM carbon grid tilted from 0° (**c**) to 45° (**d**).

therapeutic needs. With respect to our PTX co-polymer NPs, *in vitro* kinetic shows a release that is proportional to NPs co-polymer matrix degradation and depending on the total cargo, allows PTX to be released in a modulated and controlled way. This may be explained supposing PTX acts as binding agent, thus higher PTX weight content in the matrix material makes the NPs possess greater hydrophobic character, leading to limited water entry into the NPs core.

Along with *in vitro* drug release we also analyzed the degradation products of the NPs. Polyester-based NPs undergoes

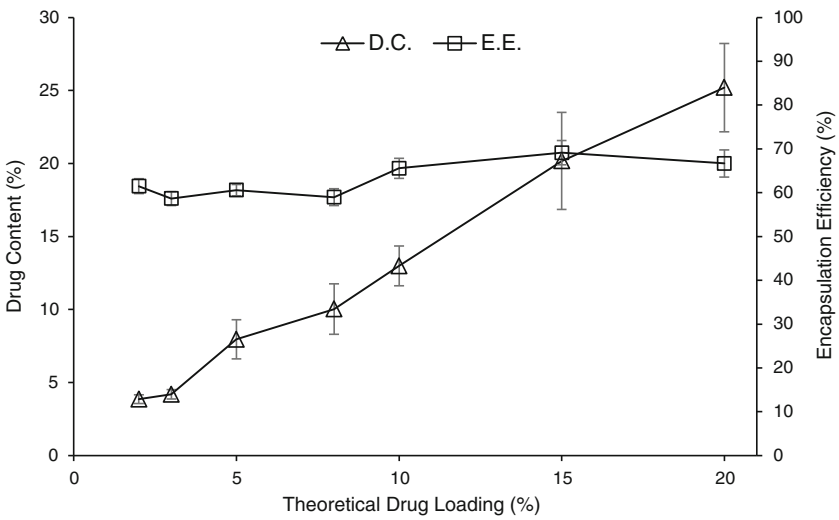

Fig. 9 Drug Content (DC % w/w) and Encapsulation Efficiency (EE %) of PTX-NPs as a function of theoretical PTX loading.

Table II NPs Recovery (%), D.C. (%) and E.E. (%) as a Function of Theoretical Drug Loading

Theoretical drug loading % (w/w)	NPs recovery (%) ± S.D.	Drug Content % (w/w) ± S.D.	Encapsulation Efficiency (w/w) %
2	49,5 ± 4.2	3,8 ± 0.2	61,5 ± 1,7
3	47,5 ± 6,1	4,2 ± 0.3	58,7 ± 1,6
5	48,2 ± 3,9	7,6 ± 1.4	60,6 ± 1,3
8	57,5 ± 6,7	10,4 ± 1.7	59 ± 1,9
10	56 ± 7,1	13,1 ± 1.3	65,6 ± 2,3
15	64,5 ± 7	19,8 ± 3.3	69,1 ± 2,8
20	60 ± 6,8	24 ± 3.5	66,7 ± 3,1

degradation by hydrolysis or biodegradation through cleavage of its backbone ester linkages into oligomers and, finally monomers. This has been demonstrated in both *in vivo* and *in vitro* (36,37). The degradation process for polyester-based NPs is mainly through uniform bulk degradation of the matrix only where the water penetration into the matrix is faster than the rate of the polymer degradation. Furthermore, the increase of carboxylic end groups as a result of biodegradation autocatalysis the process. The presence of the drug may alter the degradation mechanism combining bulk erosion with surface degradation, as well as affect the rate of matrix degradation. We studied the degradation of the NPs in terms of formation of polymer degradation products, to ensure that PTX release was related with polymer degradation, and it could not be attributed to a simple diffusion of the encapsulated drug through the polymer core matrix. Therefore, we tried to indirectly demonstrate that drug release is a good indicator of the polymer degradation. Analyzing the drug

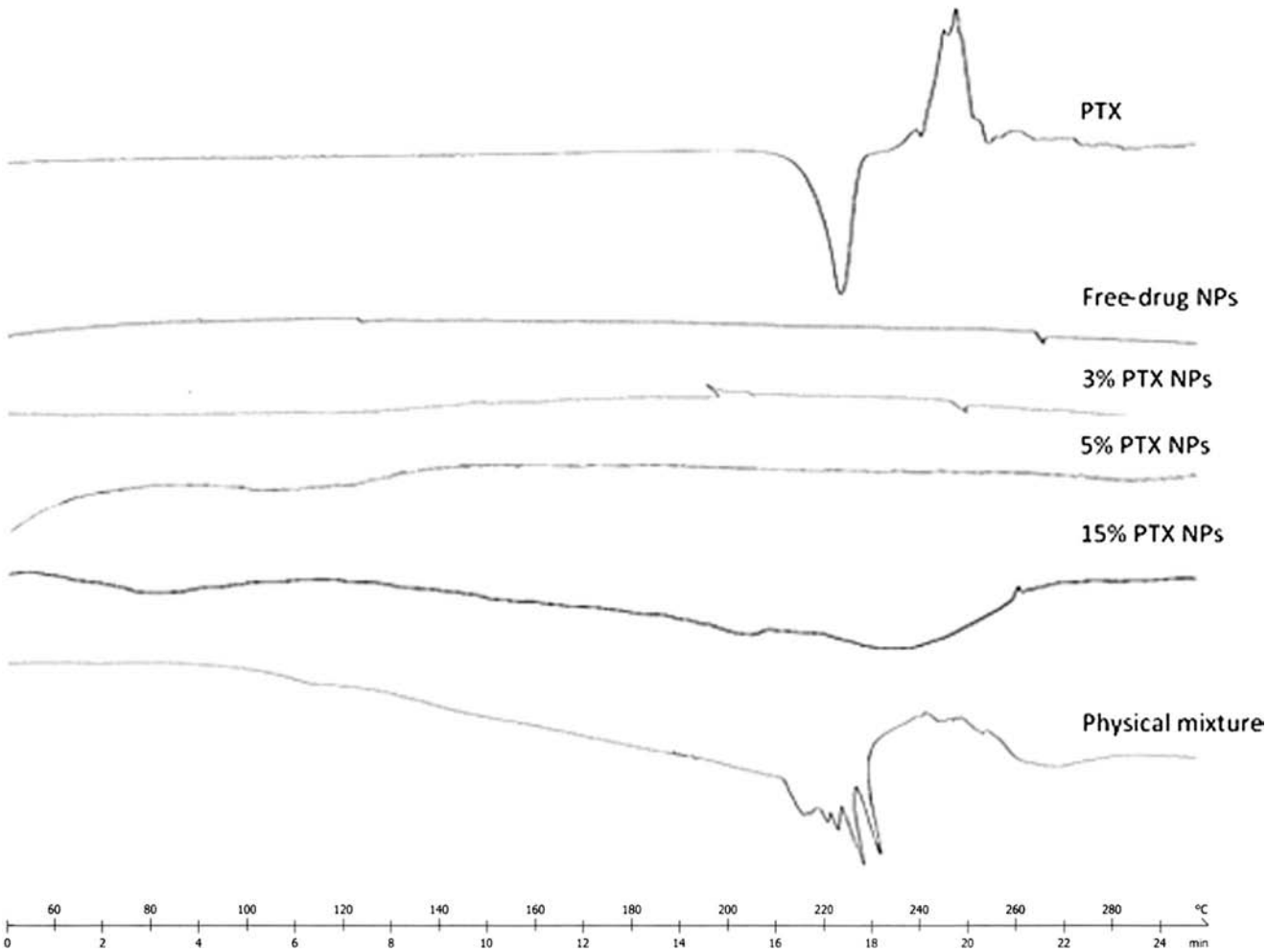

Fig. 10 Differential Scanning Calorimetry (DSC) thermographs of PTX, free-drug NPs, 3, 5, 15% PTX-NPs, and NPs/PTX as physical mixture (1:1 w/w).

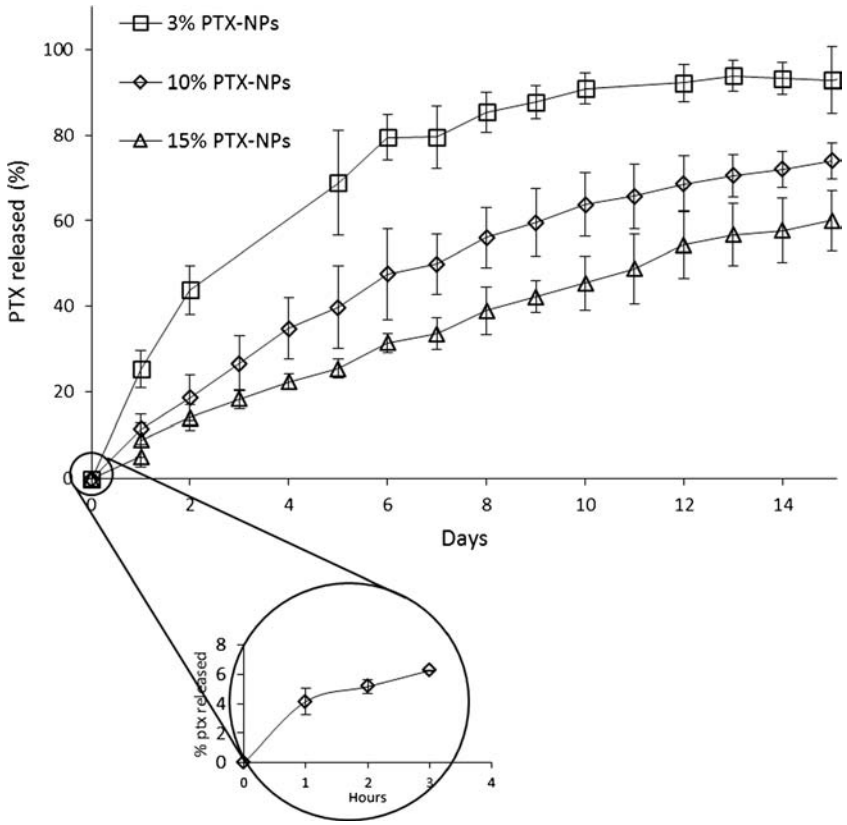

Fig. 11 *In vitro* release kinetics of PTX from P co-polymer NPs at 3, 10, 15% w/w theoretical drug content (PBS 0.1 M with 0.3% v/v Tween-80, pH 7.4, 37°C) Mean ± SD ($n = 3$).

release medium by UPLC-TOF-MS, at day 10, two groups of peaks, at high (Fig. 12) and at low molecular weight (Fig. 13) can be detected.

Analyzing the mass spectrum (Fig. 12a) the product detected at high molecular weight can be identified as PEG with a molecular weight arount 1,500 Da. This fact corroborated that PEG is one of the degradation byproducts of the polymer as expected. Also another family of peaks was identified with a molecular weight of 411.27 Da, as shown in Fig. 13. This peak was identified as the hydrophobic polymeric chain of the polymer constituting NPs (see Fig. 13) and confirms that the main mechanism of the polymer biodegradation is the hydrolysis of the polyester bond between the polyester block and the PEG moiety. These two families of degradation products were not found when the release medium was analyzed the first day of the release kinetic experiment.

Cell Experiments

In Vitro Immunological Assay

Analyzing microscopic picture of the whole blood after NPs exposure, no change in morphology is observed on RBC's, white cell and platelets (data not shown). Our results highlight that NPs and PTX-NPs are not haemolytic (<2%). In regards to cells counting, no significant change was observed in RBC's, WBC's and platelet counting at the concentration evaluated. Analyzing C3a concentration by ELISA assay, no significant activation of complement is observed in presence of the NPs suspension. Along with complement system, no relevant activation of coagulation by intrinsic or the extrinsic pathway was remarked.

In Vitro Anti-proliferative Efficiency

The *in vitro* anti-proliferative effect of drug-free NPs and PTX-NPs on U-87 MG cells was evaluated using MTS assay and PTX as comparison. As shown in Fig. 14a and b no obvious cytotoxicity was observed for the drug-free NPs. The synthetized block co-polymer (P) biocompatibility was confirmed since the drug-free NPs showed no decrease in cellular viability. Cells were incubated with 3, 5 and 8% PTX-NPs at 10 and 20 nM PTX concentrations. This range of concentrations was selected because it corresponds to plasma levels of the drug achievable in humans. As can be seen in Fig. 14a, a marked reduction in cell viability (10%) was observed when U-87 MG cells were incubated 11 days with 3% PTX-NPs at 10 nM. For the same incubation time, PTX showed similar toxicity than 3% PTX-NPs, otherwise for 5 and 8% PTX-NPs a slighter effect was observed, with 76 and 80% survival rate, respectively. With increasing PTX concentration at

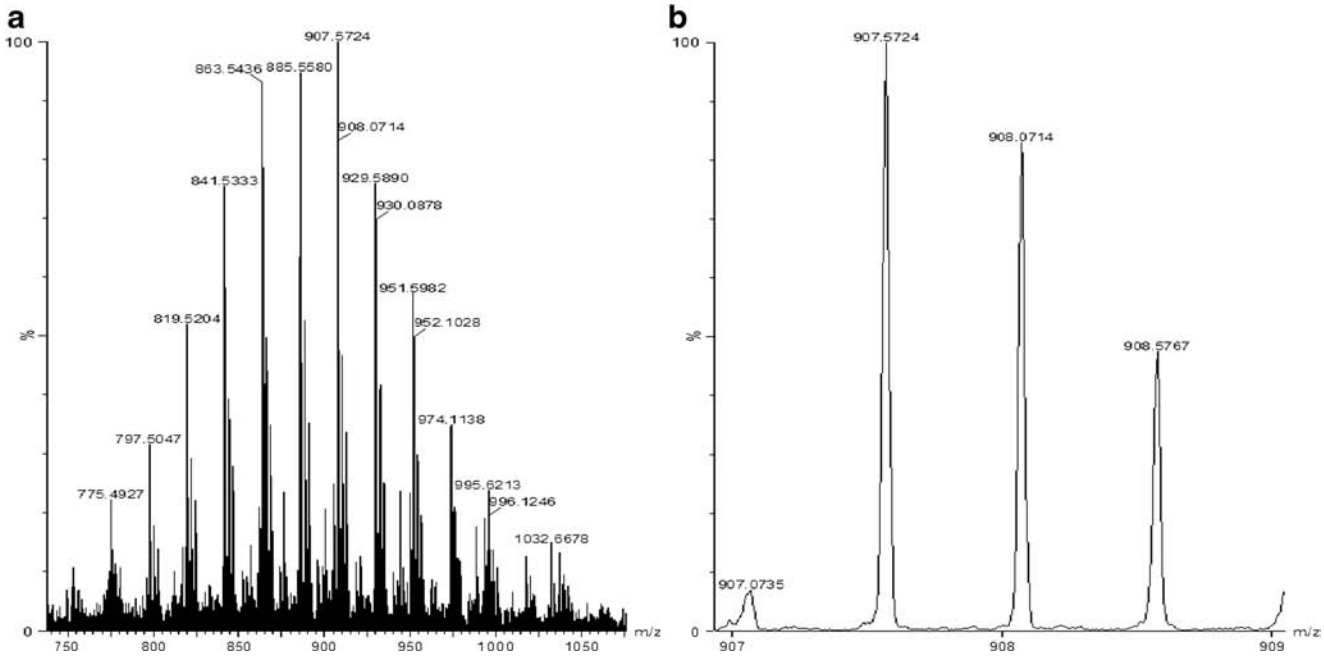

Fig. 12 UPLC-MS spectrum of release medium at day 10; (**a**) high molecular weight distribution; (**b**) spectrum zoomed on 907.5724 peak.

20 nM, a significant reduction in U-87 MG cells viability was achieved in shorter incubation times and for all formulation tested. As shown in Fig. 14b, at this concentration the cell growth was strongly inhibited after 4, 8 and 11 days for 3, 5, 8% PTX-NPs, respectively, with a reduction of approximately 50% in cell viability. Again, PTX at 20 nM showed similar effect on U-87 MG cells than 3% PTX-NPs, indicating that the developed PTX-NPs system did not decrease the PTX activity on tumoral cells and that the cytotoxicity against U87 MG cells was in time- and drug concentration-dependent manner.

Characterization of Emulsion-based PTX NPs

Emulsioned NPs showed a size of 176.4±2.5 nm with a polydispersity of 0.32±0.02 and zeta potential of −39± 1.17 mV (Table III). Unlike precipitated NPs, emulsioned NPs required lyoprotectant to assure optimal resuspension in water after freeze-drying. As shown in Table III various lyoprotectants were used and mannitol at 10% (w/v) allowed to obtain NPs with same characteristics prior to freeze-drying. Drug encapsulation studies showed an increase in drug content from 4±0.4 to 11.7±1 when the initial theoretical drug

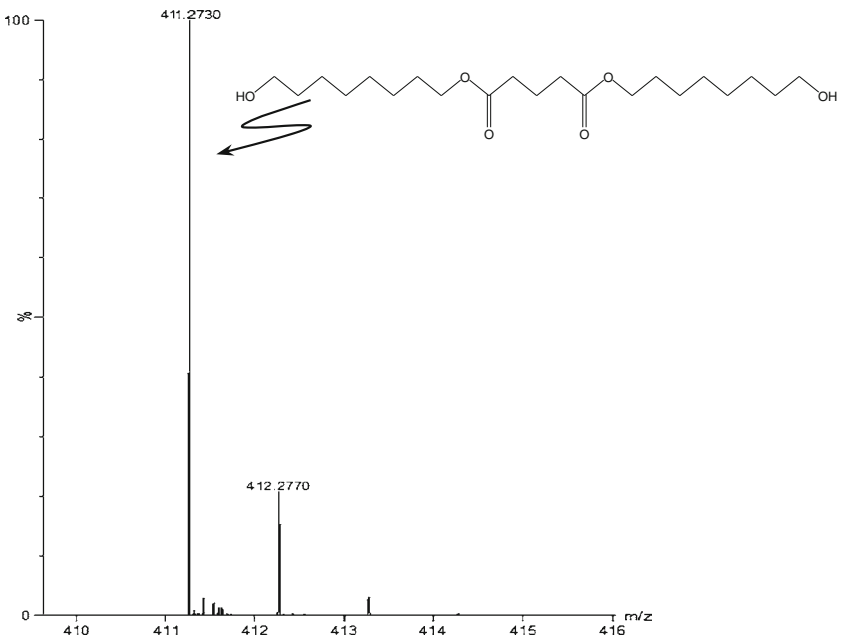

Fig. 13 UPLC-MS spectrum of release medium at day 10, low molecular weight distribution.

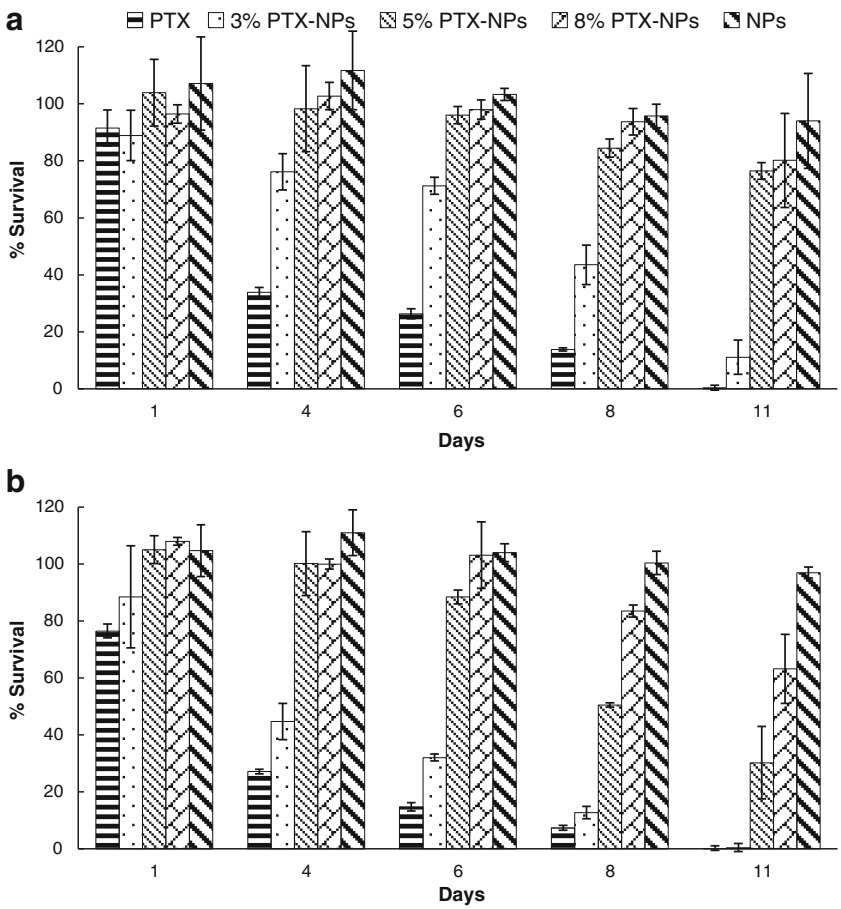

Fig. 14 Cell viability on U-87 MG incubated with PTX, NPs (drug free) and 3, 5, 8% PTXNPs at (**a**) 10 and (**b**) 20 nM PTX concentration after 11 days cell culture ($n = 3$).

loading ranged from 3 to 12%. It's important to notice that the drug content was referred to freeze-dried NPs recovered, so the values shown were not taking into account the NPs recovery yield (data not shown). The results were expressed as mean ± S.D. for three replicate samples. The results confirm the versatility of block co-polymer P and demonstrate its capacity to be employed as a drug delivery system. Indeed, satisfactory findings about size, PDI, zeta-potential and drug content were obtained by using nanoprecipitation as though emulsification-solvent evaporation techniques (Table IV).

Table III Mean Particle Size and Size Distribution (PDI) of Emulsioned NPs in the Absence or Presence of Different Lyoprotectant

Lyoprotectant used and concentration % (w/v)	Size (nm) ± S.D.	PDI ± S.D.
No freeze-dried	176,4 ± 2,5	0,32 ± 0,0
No Lyoprotectant	n.m.	1
Sucrose, 10	220,2 ± 1,1	0,31 ± 0,02
Glucose, 10	195,1 ± 5,6	0,46 ± 0,05
Lactose, 5	211,9 ± 3,4	0,24 ± 0,00
Mannitol, 10	175,5 ± 3,8	0,33 ± 0,05
Pva, 2	66,5 ± 17	0,9 ± 0,1

CONCLUSIONS

We have developed a nanoparticluate system for controlled release of anticancer drug PTX. A novel block co-polymer (P) was successfully synthetized to obtain via nanoprecipitation or emulsification-solvent evaporation method, a very monodisperse PTX-NPs population. A clear correlation between NPs characteristics and formulation parameters was found in order to entirely customize NPs in terms of size, zeta-potential, drug loading and release profile. Selected PTX-NPs showed a spherical shape with particle size of ~180 nm, polydispersity of ~0.1 and with a surrounding PEG corona on the surface. PTX content of NPs was easily increased up to 24% (w/w)

Table IV D.C. (%) of Emulsioned NPS

Theoretical Drug Loading (%, w/w)	Drug Content % (w/w) ± S.D.
3	4 ± 0.4
4	6,2 ± 0.6
8	8,2 ± 0.6
10	9,1 ± 1.1
12	11,7 ± 1

limited only by the physical state change of the drug (amorphous < 15%). High D.C. makes the system suitable for intravenous administration since no very concentrated solutions can be injected. High D.C. was probably due to strong lipophilic interactions of PTX with hydrophobic inner region of NPs. Consequently, *in vitro* PTX release from NPs, exhibiting an approximately first-order profile, depended on total cargo, with complete release approximately in 12 days for 3% theoretically loaded NPs. Higher PTX loaded NPs, limiting water entry, showed a similar trend, characterized by absence of initial burst release but with a slower release of approximately 54 and 45% for 10 and 15%, respectively, at day 9. *In vitro* cellular studies demonstrated that block co-polymer-based NPs were biocompatible, and the PTX loaded NPs had significant *in vitro* anti-tumoral activity against human primary glioblastoma cell line (U-87 MG). The cytotoxicity against U87 MG for PTX-NPs was in time- and drug concentration-dependent manner. The results appear to justify further investigation on the suitability of the system for targeting PTX-NPs through surface functionalization with target-specific ligands.

REFERENCES

1. Kawasaki ES, Player A. Nanotechnology, nanomedicine, and the development of new, effective therapies for cancer. Nanomedicine. 2005;1(2):101–9.
2. Ma Y, Zheng Y, Liu K, Tian G, Tian Y, Xu L, *et al.* Nanoparticles of poly(Lactide-Co-Glycolide)-d-a-tocopheryl polyethylene glycol 1000 succinate random copolymer for cancer treatment. Nanoscale Res Lett. 2010;5(7):1161–9.
3. Russell-Jonesa G, McTavisha K, McEwana J, Riceb J, Nowotnikb D. Vitamin-mediated targeting as a potential mechanism to increase drug uptake by tumours. J Inorg Biochem. 2004;98(10):1625–33.
4. Li Y, Pei Y, Zhang X, Gu Z, Zhou Z, Yuan W, *et al.* PEGylated PLGA nanoparticles as protein carriers: synthesis, preparation and biodistribution in rats. J Control Release. 2001;71(2):203–11.
5. Tong R, Cheng J. Ring-opening polymerization-mediated controlled formulation of polylactide-drug nanoparticles. J Am Chem Soc. 2009;131(13):4744–54.
6. Tong R, Cheng J. Paclitaxel-initiated, controlled polymerization of lactide for the formulation of polymeric nanoparticulate delivery vehicles. Angew Chem Int Ed Engl. 2008;47(26):4830–4.
7. Essa S, Rabanel JM, Hildgen P. Effect of polyethylene glycol (PEG) chain organization on the physicochemical properties of poly(D, L-lactide) (PLA) based nanoparticles. Eur J Pharm Biopharm. 2010;75(2):96–106.
8. Moghimi SMDS. Innovations in avoiding particle clearance from blood by Kupffer cells: cause for reflection. Crit Rev Ther Drug Carrier Syst. 1994;11(1):31–59.
9. Moghimi SM, Porter CJ, Muir IS, Illum LDS. Non-phagocytic uptake of intravenously injected microspheres in rat spleen: influence of particle size and hydrophilic coating. Biochem Biophys Res Commun. 1991;177(2):861–6.
10. Moghimi SM, Hunter AC, Murray JC. Nanomedicine: current status and future prospects. FASEB J. 2005;19(3):311–30.
11. Hamblett KJ, Senter PD, Chace DF, Sun MMC, Lenox J, Cerveny CG, *et al.* Effects of drug loading on the antitumor activity of a monoclonal antibody drug conjugate effects of drug loading on the antitumor activity of a monoclonal antibody drug conjugate. Clin Cancer Res. 2004;10:7063–70.
12. Zhou S, Xu J, Yang H, Deng X. Synthesis and characterization of biodegradable poly(e-caprolactone)-polyglycolide-poly(ethylene glycol) monomethyl ether random copolymer. Macromol Mater Eng. 2004;289:576–80.
13. Cheng J, Teply BA, Sherifi I, Sung J, Luther G, Gu FX, *et al.* Formulation of functionalized PLGA-PEG nanoparticles for in vivo targeted drug delivery. Biomaterials. 2007;28(5):869–76.
14. Couvreur P, Dubernet C, Puisieux F. Controlled drug delivery with nanoparticles: current possibilities and future trends. Eur J Pharm Biopharm. 1995;41(1):2–13.
15. Fessi H, Puisieux F, Devissaguet JP, Ammoury N, Benita S. Nanocapsule formation by interfacial polymer deposition following solvent displacement. Int J Pharm. 1989;55(1):R1–4.
16. Bilati U, Allémann E, Doelker E. Development of a nanoprecipitation method intended for the entrapment of hydrophilic drugs into nanoparticles. Eur J Pharm Sci. 2005;24(1):67–75.
17. Musumeci T, Ventura CA, Giannone I, Ruozi B, Montenegro L, Pignatello R, *et al.* PLA/PLGA nanoparticles for sustained release of docetaxel. Int J Pharm. 2006;325(1–2):172–9.
18. Soppimath KS, Aminabhavi TM, Kulkarni AR, Rudzinski WE. Biodegradable polymeric nanoparticles as drug delivery devices. J Control Release. 2001;70(1–2):1–20.
19. Gelderblom H, Verweij J, Nooter K, Sparreboom A. Cremophor EL: the drawbacks and advantages of vehicle selection for drug formulation. Eur J Cancer. 2001;37(13):1590–8.
20. Spratlin JSM. Pharmacogenetics of paclitaxel metabolism. Crit Rev Oncol Hematol. 2007;61(3):222–9.
21. Marcel Musteata F, Pawliszyn J. Determination of free concentration of paclitaxel in liposome formulation. J Pharm Pharm Sci. 2006;9:231–7.
22. Kim SY, Shin IG, Lee YM, Cho CS, Sung YK. Methoxy poly(ethylene glycol) and epsilon-caprolactone amphiphilic block copolymeric micelle containing indomethacin. II. Micelle formation and drug release behaviours. J Control Release. 1998;51(1):13–22.
23. Averineni RK, Shavi GV, Gurram AK, Deshpande PB, Arumugam K, Maliyakkal N, *et al.* PLGA 50:50 nanoparticles of paclitaxel: development, in vitro anti-tumor activity in BT-549 cells and in vivo evaluation. Bull Mater Sci. 2012;35(3):319–26.
24. Budhian A, Siegel SJ, Winey KI. Haloperidol-loaded PLGA nanoparticles: systematic study of particle size and drug content. Int J Pharm. 2007;336(2):367–75.
25. Senichev VY, Tereshatov VV. General principles governing dissolution of materials in solvents. In: Wypych G, editor. Handbook of solvents. 2001. p. 101–214.
26. Thioune O, Fessi H, Devissaguet JP, Puisieux F. Preparation of pseudolatex by nanoprecipitation: influence of the solvent nature on intrinsic viscosity and interaction constant. Int J Pharm. 1997;146(2):233–8.
27. Mu L, Feng SS. Vitamin E TPGS used as emulsifier in the solvent evaporation/extraction technique for fabrication of polymeric nanospheres for controlled release of paclitaxel (Taxol). J Control Release. 2002;80(1–3):129–44.
28. Fonseca C, Simões S, Gaspar R. Paclitaxel-loaded PLGA nanoparticles: preparation, physicochemical characterization and in vitro anti-tumoral activity. J Control Release. 2002;83(2):273–86.
29. Danhier F, Lecouturier N, Vroman B, Jérôme C, Marchand-Brynaert J, Feron O, *et al.* Paclitaxel-loaded PEGylated PLGA-based nanoparticles: in vitro and in vivo evaluation. J Control Release. 2009;133(1):11–7.
30. Gaucher G, Marchessault RH, Leroux J-C. Polyester-based micelles and nanoparticles for the parenteral delivery of taxanes. J Control Release. 2010;143(1):2–12.

31. Hu Q, Gao X, Gu G, Kang T, Tu Y, Liu Z, *et al.* Glioma therapy using tumor homing and penetrating peptide-functionalized PEG-PLA nanoparticles loaded with paclitaxel. Biomaterials. 2013;34(22):5640–50.
32. Hu Q, Gu G, Liu Z, Jiang M, Kang T, Miao D, *et al.* F3 peptide-functionalized PEG-PLA nanoparticles co-administrated with tLyp-1 peptide for anti-glioma drug delivery. Biomaterials. 2013;34(4):1135–45.
33. Wang G, Yu B, Wu Y, Huang B, Yuan Y, Liu CS. Controlled preparation and antitumor efficacy of vitamin E TPGS-functionalized PLGA nanoparticles for delivery of paclitaxel. Int J Pharm. 2013;446(1–2):24–33.
34. Mu L, Feng S-S. PLGA/TPGS nanoparticles for controlled release of paclitaxel: effects of the emulsifier and drug loading ratio. Pharm Res. 2003;20(11):1864–72.
35. Xin H, Chen L, Gu J, Ren X, Wei Z, Luo J, *et al.* Enhanced anti-glioblastoma efficacy by PTX-loaded PEGylated poly(ε-caprolactone) nanoparticles: in vitro and in vivo evaluation. Int J Pharm. 2010;402(1–2):238–47.
36. Ramchandani M, Robinson D. In vitro and in vivo release of ciprofloxacin from PLGA 50:50 implants. J Control Release. 1998;54(2):167–75.
37. Amann LC, Gandal MJ, Lin R, Liang Y, Siegel SJ. In vitro-in vivo correlations of scalable PLGA-risperidone implants for the treatment of schizophrenia. Pharm Res. 2010;27(8):1730–7.